

Light scattering observations of spin reversal excitations in the fractional quantum Hall regime

Irene Dujovne,^{1,2} C.F. Hirjibehedin,^{3,2} A. Pinczuk,^{1,2,3}
Moonsoo Kang,⁴ B.S. Dennis,² L.N. Pfeiffer,² and K.W. West²

¹*Department of Applied Physics and Applied Math, Columbia University, New York, NY 10027*

²*Bell Labs, Lucent Technologies, Murray Hill, NJ 07974*

³*Department of Physics, Columbia University, New York, NY 10027*

⁴*Physics Department, Washington State University, WA 99164-2814.*

(Dated: January 12, 2022)

Resonant inelastic light scattering experiments access the low lying excitations of electron liquids in the fractional quantum Hall regime in the range $2/5 \geq \nu \geq 1/3$. Modes associated with changes in the charge and spin degrees of freedom are measured. Spectra of spin reversed excitations at filling factor $\nu \gtrsim 1/3$ and at $\nu \lesssim 2/5$ identify a structure of lowest spin-split Landau levels of composite fermions that is similar to that of electrons. Observations of spin wave excitations enable determinations of energies required to reverse spin. The spin reversal energies obtained from the spectra illustrate the significant residual interactions of composite fermions. At $\nu = 1/3$ energies of spin reversal modes are larger but relatively close to spin conserving excitations that are linked to activated transport. Predictions of composite fermion theory are in good quantitative agreement with experimental results.

PACS numbers: 73.20.Mf, 73.43.Lp, 73.43.Nq

The fractional quantum Hall effect (FQHE) is an electron condensation phenomenon that occurs at low temperatures when two-dimensional electron systems of very low disorder are exposed to high magnetic fields. The FQH states are archetypes of quantum fluids that emerge in low dimensional electron systems due to the impact of fundamental interactions. In the FQHE the 2D electron system becomes incompressible at certain values of the Landau level filling factor $\nu = nhc/eB$, where n is the electron density and B is the perpendicular magnetic field. In the filling factor range $1 \geq \nu \geq 1/3$ the major sequence of the FQHE occurs at ‘magic’ filling factors $\nu = p/(2p \pm 1)$, where p is an integer. The composite fermion (CF) framework interprets the sequence by attaching two vortices of the many body wavefunction to each electron [1, 2]. Chern-Simons gauge fields incorporate electron interactions so that CF’s experience effective magnetic fields $B^* = B - B_{1/2} = \pm B/(2p \pm 1)$, where $B_{1/2}$ is the perpendicular magnetic field at $\nu = 1/2$ [3, 4, 5]. Composite fermion quasiparticles have spin-split energy levels characteristic of charged fermions with spin $1/2$ moving in the effective magnetic field B^* . The levels resemble spin-split Landau levels of electrons. The number p thus becomes the CF Landau level filling factor and in FQHE states at $\nu = p/(2p \pm 1)$ there are p fully occupied levels of composite fermions.

Structures of spin-split CF levels are shown schematically in Fig. 1 for $\nu \gtrsim 1/3$ and $\nu \lesssim 2/5$. The spacing between sequential CF levels with same spin is represented as a cyclotron frequency [3, 6, 7, 8, 9, 10, 11, 12], $\omega_c = eB^*/cm_{CF}$, where m_{CF} is a CF effective mass. Figure 1 also presents the transitions of composite fermions near filling factors $1/3$ and $2/5$. The charge mode (CM) transitions are spin-conserving. The spin wave (SW) and spin flip (SF) transitions involve a spin-reversal. The CM

transition energies, however, could be different from CF level spacings. The difference is due to the changes in self-interaction energies that may occur when quasiparticles and quasiholes are created [9].

Neutral pair excitations of quasiparticles above FQHE ground states are constructed from transitions such as those shown in Fig. 1. The excitations are described as modes that have characteristic energy vs. wave vector dispersions $\omega(q)$ [13, 14, 15]. The separation between the neutral quasiparticle-quasihole pairs is $x_o = ql_o^2$, where $l_o = (\hbar c/eB)^{1/2}$ is the magnetic length. The Coulomb energy $E_c = e^2/\epsilon l_o$, where ϵ is the dielectric constant of the host semiconductor ($\epsilon = 12.6$ in GaAs) defines the energy scale for the excitations. Salient features of the dispersions are at critical points. The critical points occur at $q \rightarrow 0$, at the $q \rightarrow \infty$ limit and at roton minima at finite wavevector. These roton minima, known as magnetorotons, are due to excitonic binding interactions in neutral quasiparticle-quasihole pairs with $q \simeq 1/l_o$. The mode at large wavevector ($q \rightarrow \infty$) represents a non-interacting quasiparticle-quasihole pair at large separation [3].

Composite fermion quasiparticles are expected to experience interactions that are much weaker than those among electrons. This occurs because Chern-Simons gauge fields linked to vortex attachment in forming CF quasiparticles incorporate significant Coulomb interactions. The energy differences between critical points, such as that between the magnetoroton and the large wave vector ($q \rightarrow \infty$) CM excitations, being manifestations of residual interactions, provide experimental venues to test key predictions of the composite fermion approach.

The critical points of dispersions of spin and charge collective modes of the FQH liquid are accessed in resonant inelastic light scattering experiments [16, 17, 18, 19,

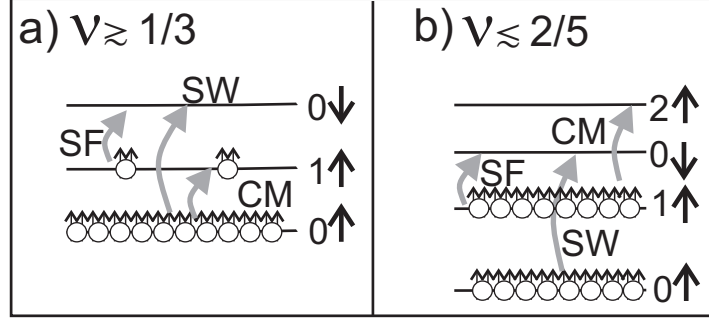


FIG. 1: Structure of spin-split Landau levels of CFs that interpret the low lying excitations observed in this work. (a) $\nu \gtrsim 1/3$. (b) $\nu \lesssim 2/5$. Landau levels are labelled by quantum numbers and arrows that indicate orientation of spin. The lowest SF, SW and CM transitions are depicted. Composite fermions are shown as small circles with two arrows that represent the two vortices attached to each electron.

20, 21]. Results at $\nu = 1/3$ have determined the energies of rotons at $q \sim 1/l_o$, and of large wave vector ($q \rightarrow \infty$) excitations of the spin conserving CM transitions [22]. The observed energy splitting between rotons at Δ_R and $q \rightarrow \infty$ modes at Δ_∞ , by light scattering measurements, is direct evidence of the strength of residual CF interactions. CF evaluations of dispersions of quasiparticle excitations are in good quantitative agreement with light scattering results [22, 23].

In more recent light scattering experiments quasiparticle excitations in the spin and charge degrees of freedom have been observed in the full range $2/5 \geq \nu \geq 1/3$ [24, 25]. The measured excitations are interpreted with transitions CM, SW and SF. The results suggest that CF quasiparticles have the well defined structure of spin-split CF Landau levels shown in Fig 1. The dependence of the measured mode energies on filling factor in the range $2/5 \geq \nu \geq 1/3$ indicate significant residual interactions among the quasiparticles.

We report here inelastic light scattering studies of spin excitations of the electron liquid at filling factors $1/3 \leq \nu \leq 2/5$. Two distinct types of spin modes are considered: spin waves and spin flip excitations based on the correspondingly labelled transitions shown in Fig.1. In spin waves there is only spin reversal, while in spin flip modes spin and CF Landau level quantum number change simultaneously.

The light scattering measurements of spin excitations yield direct determinations of spin-reversal energies of quasiparticles of the FQH liquids. The results reveal large spin reversal energies that are due to residual quasiparticle interactions [26, 27, 28, 29, 30]. In conjunction with determinations of CM transitions the light scattering measurements of spin excitations represent unique experimental tests of composite fermion theory. These large residual CF interactions are possibly linked to those that manifest in condensation of composite fermions into higher order liquid states [31, 32, 33].

At filling factor $1/3$ we identify the large wavevector

limit ($q \rightarrow \infty$) of the spin wave energy E_Z^* at

$$E_Z^* = E_Z + E^{\uparrow\downarrow} \quad (1)$$

where $E^{\uparrow\downarrow}$ represents the spin reversal energy due to interactions among quasiparticles [26, 27, 28, 29, 30]. The bare Zeeman energy is $E_Z = g\mu_B B_T$, where B_T is the total magnetic field, μ_B is the Bohr magneton and $g \sim 0.44$ is the absolute value of the Lande factor of GaAs. A peak at E_Z that occurs in the light scattering spectra is interpreted as the $q \rightarrow 0$ limit of the SW mode (Larmor's theorem) [13]. The light scattering observations of SW modes at large wave vector ($q \rightarrow \infty$) at E_Z^* reported here allow the direct determination of $E^{\uparrow\downarrow}$.

A determination of $E^{\uparrow\downarrow}$ was reported in Ref. [24] from the energy of $|1 \uparrow\rangle \rightarrow |0 \downarrow\rangle$ transitions that occur when the second CF Landau level begins to populate at $\nu \gtrsim 1/3$. In Ref. [24] the simultaneous measurements of E_Z , the CM collective mode at Δ_∞ and the newly discovered SF mode enabled a preliminary determination of the many-body spin reversal energy. Both Δ_∞ and $E^{\uparrow\downarrow}$ are linear in the Coulomb energy E_c . The value of $E^{\uparrow\downarrow} \cong 0.054E_c$ has been reported. The alternate determination of $E^{\uparrow\downarrow}$ from large wave vector ($q \rightarrow \infty$) SW modes reported here is in excellent agreement with the previous result.

In the present study we find that Δ_∞ is smaller but close to the determined value of E_Z^* . Δ_∞ , the energy of a widely separated spin conserving quasiparticle quasi-hole pair, is linked to the activation energy that determines the temperature dependence of longitudinal magnetotransport. The result showing that Δ_∞ and E_Z^* have similar energy implies that spin excitations could play a role in temperature activated processes and explain some of the discrepancies between experimental and calculated activation energies [7, 30].

In the composite fermion framework the interplay between spin reversal energies and level spacings dictates the spin polarization of the liquid states. In this competition between the two energies the small Zeeman energy can play a pivotal role. For example, states such as $2/5$,

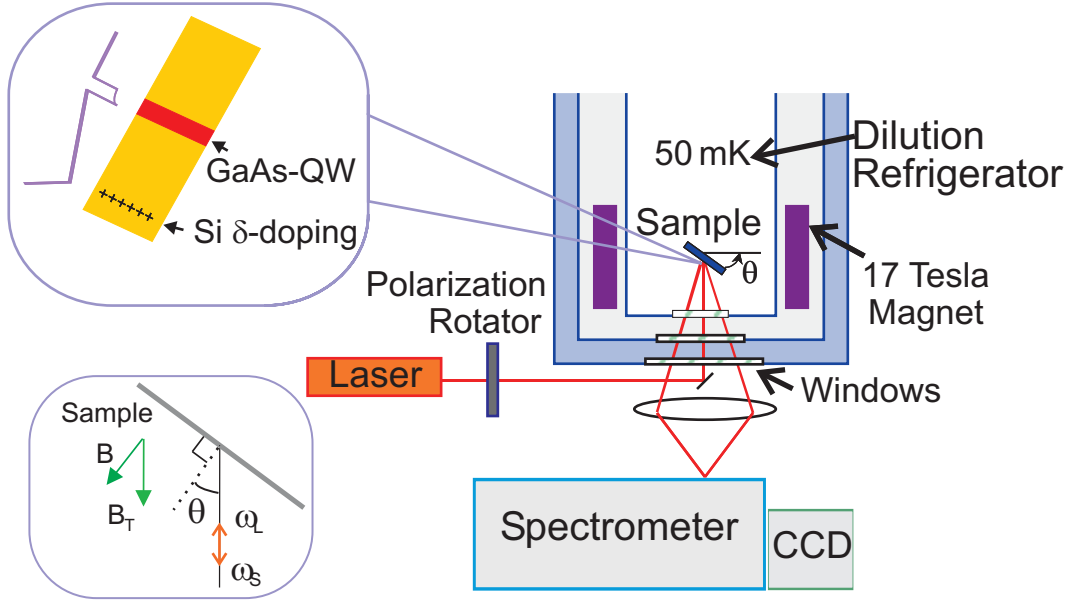


FIG. 2: Schematic description of light scattering experiments at millikelvin temperatures. The top inset depicts quantum layers and the bottom of conduction. The lower inset shows the backscattering arrangement for the sample and the orientation of the magnetic field.

with two CF Landau levels fully populated (as seen in Fig. 1), are spin-polarized because at relatively large fields E_Z is larger than the difference between the level spacing and the spin reversal energy due to interactions. The interaction term of the spin reversal energy, $E^{\uparrow\downarrow}$, depends on the spin polarization of the FQH states. Light scattering determinations of spin reversal energies could offer venues to probe spin polarizations of states with $\nu > 1/3$.

The resonant inelastic light scattering experiments are carried out with photon energies that overlap fundamental optical transitions of the semiconductor quantum structure that hosts the 2D system. Conservation of energy in the inelastic scattering processes is expressed as $\omega(q) = \pm(\omega_L - \omega_S)$, with \pm corresponding to the Stokes and anti-Stokes processes respectively. The in-plane inelastic scattering wavevector, \mathbf{k}_{\parallel} , is such that $|\mathbf{k}_{\parallel}| = k_{\parallel} = (k^L - k^S)\sin\theta \sim (2\omega_L/c)\sin\theta$, where L and S refer to incident (laser) and scattered wavevectors of light and θ is the tilt angle. The backscattering configuration shown in Fig 2 offers access to in-plane wavevectors $k_{\parallel} \sim 10^5 \text{ cm}^{-1}$ and $k_{\parallel}l_o \lesssim 0.1$. Conservation of momentum for systems with translational invariance is equivalent to conservation of wavevector. In 2D systems this converts to $\mathbf{q} = \mathbf{k}_{\parallel}$. Wavevector conservation breaks down with the loss of full translation symmetry in the presence of weak residual disorder that occurs even in systems of high perfection. In this case the light scattering spectra will display the contributions from the critical points in the density of states [17, 18, 34, 35].

The high quality 2D electron system in each sample resides in single GaAs quantum well (SQW) of typical width $d = 330 \text{ \AA}$. We present results from samples

with density $n = 5.6 \times 10^{10} \text{ cm}^{-2}$ and $7.6 \times 10^{10} \text{ cm}^{-2}$. The electron mobilities are very high, reaching a value $\mu \gtrsim 7 \times 10^6 \text{ cm}^2/\text{Vsec}$ at $T \cong 300 \text{ mK}$. The samples were mounted on the cold finger of a $^3\text{He}/^4\text{He}$ dilution refrigerator that is inserted in the cold bore of a superconducting magnet with windows for optical access (see Fig. 2). Cold finger temperatures are variable and as low as 45 mK. The resonant inelastic light spectra were excited with a diode laser with photon energies ω_L close to the fundamental optical gap of the GaAs SQW. The power density was kept below 10^{-4} W/cm^2 . The spectra were acquired with a double Czerny-Turner spectrometer operating in additive mode and a CCD camera with $15 \text{ }\mu\text{m}$ pixels. The combined resolution with a $30 \text{ }\mu\text{m}$ slit is 0.016 meV .

We measured depolarized spectra with orthogonal incident and scattered light polarizations and polarized spectra in which polarizations are parallel. Excitation modes with changes in the spin degree of freedom tend to be stronger in depolarized spectra, while modes in the charge degree of freedom tend to be stronger in polarized spectra. A backscattering geometry shown in the inset to Fig. 2 was used with an angle $\theta \sim 30^\circ$. The perpendicular component of magnetic field is $B = B_T \cos\theta$, where B_T is the total field.

Figure 3 displays depolarized spectra at filling factors $\nu \gtrsim 1/3$. The spectra show the long wavelength SW at E_Z and a weaker narrow peak, labelled SF^+ , that occurs at lower energies. The intensity of the new peak depends strongly on filling factor. It is absent for $\nu = 1/3$ and its intensity increases as the field is decreased towards higher filling factors, indicating that this mode is related to the population of the second Landau level $|1 \uparrow\rangle$. On

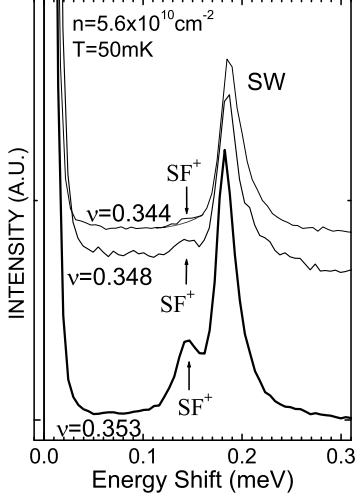


FIG. 3: Depolarized inelastic light scattering spectra at filling factors $\nu \gtrsim 1/3$. Vertical arrows show the peak assigned to the spin-flip mode

this basis this mode was assigned to the SF transition $|1 \uparrow\rangle \rightarrow |0 \downarrow\rangle$ shown in Fig. 1 [24].

Figure 4(a) displays spectra taken at $\nu = 1/3$. Four of the excitations shown in Fig. 4(a) have been assigned in Ref. [22]. SW is the long wavelength ($q \rightarrow 0$) spin wave mode at E_z . The other three are CM modes: Δ_R is the magnetoroton, Δ_0 is the $q \rightarrow 0$ mode, and Δ_∞ the large wavevector mode. The assignments are consistent with the calculated dispersions of CM modes shown in Fig. 4(b)[22, 23]. There is a fifth mode that has not been previously reported. It appears at an energy of 0.83meV, between Δ_0 and Δ_∞ . It is natural to assign this mode to the critical point of spin wave excitations that occurs at large wavevectors. Its energy is indicated as E_z^* (see Eq. 1). This assignment enabled us to construct the schematic rendition of the spin wave dispersion shown by the dotted line curve in Fig 4(b).

The spin flip excitation labelled SF^+ in Fig. 3 occurs at $\nu \gtrsim 1/3$, when there is only very low population of the $|1 \uparrow\rangle$ level. The mode is represented by the SF transitions shown in Fig. 1. Its energy is approximated as [24]

$$E_{SF} = E_Z + E^{\uparrow\downarrow} - \Delta_\infty \quad (2)$$

The value $\Delta_\infty = 0.059E_c$ was obtained from the CM mode at large q shown in Fig. 4(a). The bare Zeeman energy was obtained from spectra such as those in Figs. 3 and 4(a), where E_Z is given by the position of the peaks labeled SW. With these determinations it was found that $E^{\uparrow\downarrow} \cong 0.054E_c$ [24].

The measurement of the total spin reversal energy E_Z^* from the spin wave mode at $q \rightarrow \infty$, as shown in Fig. 4, provides a second determination of the many-body term of the spin reversal energy $E^{\uparrow\downarrow}$. From $E_Z^* = 0.83\text{meV}$

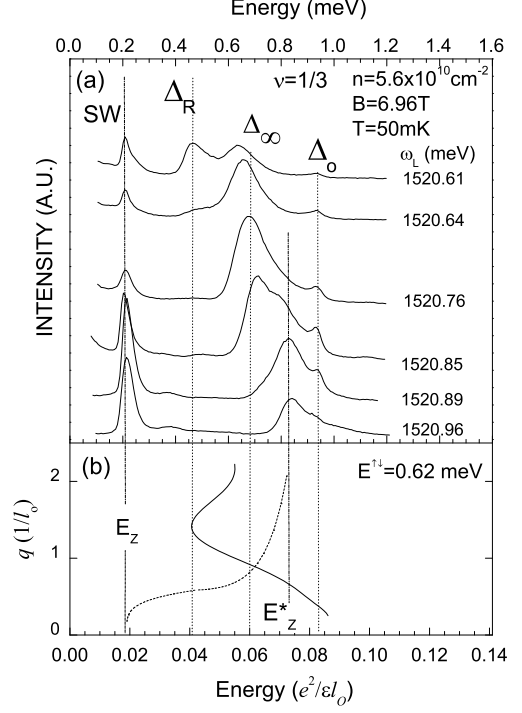


FIG. 4: (a) Resonant inelastic light scattering spectra at $\nu=1/3$. The incident photon energies are indicated in meV. The mode labelled SW is the $q = 0$ spin wave excitation at E_z . Δ_R is the CM roton and Δ_0 is the CM mode at $q = 0$. The large wavevector limit ($q \rightarrow \infty$) of the CM mode is at Δ_∞ . E_z^* is the large wavevector limit ($q \rightarrow \infty$) of the spin wave mode. (b) The thick line is the dispersion of the CM excitation (after Scarola et al. [23]). The dotted line is a schematic representation for the spin wave dispersion.

and $E_Z = 0.21\text{meV}$ we obtain $E^{\uparrow\downarrow} = 0.62\text{ meV} = 0.053E_c$, identical within the experimental uncertainty to the value of $E^{\uparrow\downarrow}$ obtained from measurements of E_{SF} . This consistency between the two independently obtained values testifies to the significant reliability of the determinations of E_Z^* and $E^{\uparrow\downarrow}$ from light scattering spectra at $\nu \gtrsim 1/3$.

Figure 5 shows spectra of low lying spin excitation modes at filling factors in the range $2/5 \geq \nu \geq 1/3$. The results in panel (a) are from the sample with density $7.6 \times 10^{10} \text{ cm}^{-2}$. The spectra in panel (b), from the sample with density $5.6 \times 10^{10} \text{ cm}^{-2}$, are those reported in Ref. [24]. Although there is considerable difference in density, both samples show a similar behavior. The figure reveals that an excitation derived from the SF roton at $\nu = 2/5$ [11, 24], the mode labelled SF^- , shifts to lower energies as the second level starts to depopulate for $\nu \lesssim 2/5$, and disappears for filling factors in the middle of the range $2/5 \geq \nu \geq 1/3$. At larger magnetic fields, $\nu \gtrsim 1/3$, a narrow peak (SF^+) appears below the SW. This peak, also displayed in Fig. 3, disappears as the

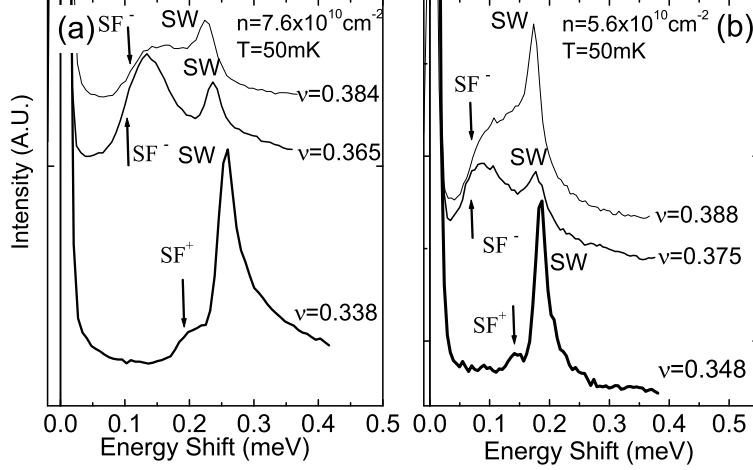


FIG. 5: Inelastic light scattering measurements at different filling factors $1/3 \geq \nu \geq 2/5$ for two densities (a) $7.6 \times 10^{10} \text{ cm}^{-2}$ and (b) $5.6 \times 10^{10} \text{ cm}^{-2}$. Vertical arrows show the peaks assigned to the SF modes (SF^- and SF^+)

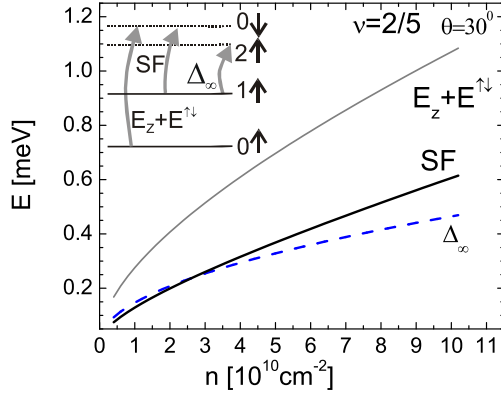


FIG. 6: Evaluations of the energies of the large wavevector limits of the spin wave at $E_z + E^{\uparrow\downarrow}$, of the CM mode at Δ_∞ and of the spin flip (SF) modes as function of density for $\nu = 2/5$ and $\theta = 30^\circ$. The inset shows the lowest CF levels. Fully populated levels are depicted as full lines. Empty levels are shown as dotted lines.

state with $\nu = 1/3$ is approached. The results at $\nu \gtrsim 1/3$ in Fig. 5(a) enable determinations of $E^{\uparrow\downarrow}$ with Eq. 2. We find a square root dependence on perpendicular field given by $E^{\uparrow\downarrow} \cong 0.054 E_c$ at both densities.

The values of Δ_∞ , $E^{\uparrow\downarrow}$ and E_z determined at $\nu = 1/3$ are employed to estimate the density dependence of the low-lying spin and charge excitations at $\nu = 1/3$ and $\nu = 2/5$. The linear dependence of Δ_∞ and $E^{\uparrow\downarrow}$ on E_c translates into a square root dependence on density. For each value of density we assume that the CM energy

at large wavevector for $\nu = 2/5$ is given by the simple scaling $\Delta_\infty(2/5) = \Delta_\infty/2$.

Figure 6 displays evaluations of the energies of low-lying spin and charge excitations as function of density for an angle $\theta = 30^\circ$ at filling factor $\nu = 2/5$ ($p = 2$). The figure shows the large wave vector spin wave energy $E_z + E^{\uparrow\downarrow}$, $\Delta_\infty(2/5)$ and the energy of the large wave vector spin-flip mode (SF). The values obtained for the SF energy are in excellent agreement to the composite fermion evaluations by Mandal and Jain at [11, 30]. On the other hand our values $\Delta_\infty(2/5)$ are lower than those in Ref. [30].

One of the intriguing issues to consider further is that of the relation between SF modes and the spin polarization of the $2/5$ state. A loss of spin polarization in the $2/5$ state was reported in transport experiments with tunable Zeeman energy and in luminescence determinations as function of density [36, 37]. Recently a roton in the dispersion of SF excitations was discovered [11, 24]. It is conceivable that the loss of polarization is related to a roton instability of SF excitations that occurs when E_z collapses either at small densities or small g factor.

Similar evaluations of the density dependence of the Δ_∞ , E_z^* and $E^{\uparrow\downarrow}$ energies evaluated at $\nu = 1/3$ are presented in Fig. 7. The finding that Δ_∞ is relatively close to E_z^* confirms that the bare Zeeman energy plays the key role in setting up the hierarchy of the lowest CF levels and excitations at $q \rightarrow \infty$. We recall that Δ_∞ is considered to be the activation energy measured in magnetotransport. The closeness of Δ_∞ and E_z^* , shown Fig. 7, suggest that spin reversal excitations represented by E_z^* could have a non trivial impact on charge transport at $\nu = 1/3$.

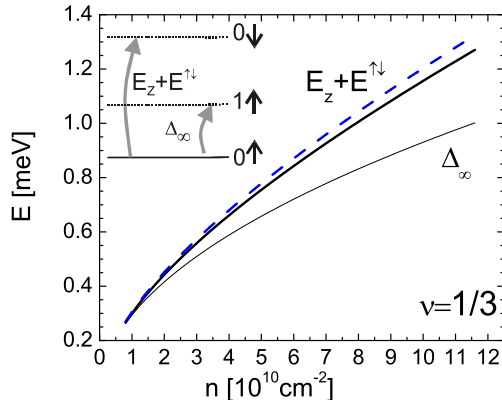


FIG. 7: Evaluations at $\nu = 1/3$ of large wavevector limit of the SW (thick line), spin reversal energy and Δ_∞ (thin line) as a function of density. The large wavevector limit of the spin wave is calculated at 30° (dashed line) and 0° (solid line). The inset shows the lowest CF levels. Fully populated levels are shown as full lines. Empty levels are represented as dotted lines.

The results for Δ_∞ in Fig. 7 have played a key role in the determination of spin reversal energies [24]. Δ_∞ can be represented by a cyclotron frequency with CF cyclotron mass m_{CF} that is a function of $n^{1/2}$. For the two samples of this study we find masses of $0.39m_e$ and $0.45m_e$ for the densities 5.6 and $7.6 \times 10^{10} \text{ cm}^{-2}$ respectively. At $n = 1.1 \times 10^{11} \text{ cm}^{-2}$ the $n^{1/2}$ dependence of the cyclotron mass yields a value $m_{CF} = 0.54m_e$, that is somewhat smaller, but close, than determinations of m_c from activated magnetotransport [7].

The results presented in this paper show that light scattering experiments offer direct access to key features of low-lying excitations in the spin and charge degrees of freedom in the FQH regime. Near $2/5$ and $1/3$ the spectra offer evidence of spin-split CF Landau levels of charged fermions with spin $1/2$. Spin-reversal energies, associated with spin waves and spin flip excitations, are readily determined from the spectra. Current evaluations of spin-reversed quasiparticle excitations are in excellent quantitative agreement with our results. The spin reversal energies, typically about one fifth of that for electrons at $\nu = 1$ [38], indicate significant residual CF interactions. These residual interactions could interpret condensed states at filling factors in the range $2/5 > \nu > 1/3$ with partial population of CF Landau levels [32, 39, 40].

Inelastic light scattering methods at low temperatures in the 100mK range and below have enormous potential to probe the impact of fundamental interactions of two dimensional electron systems in the FQH regimes. By giving unique access to low lying spin reversal excitation light scattering experiments can study the spin polarization of the liquid states. Determinations of $\Delta_\infty(\nu)$ when compared with the corresponding activation energies in magnetotransport will enable assessments of mechanisms for charge transport. Further studies of low lying modes could offer unprecedented insights into quantum phases of the low-dimensional electron system.

We are grateful to H. L. Stormer for discussions on this work. This work was supported in part by the Nanoscale Science and Engineering Initiative of the National Science Foundation under NSF Award Number CHE-0117752 and by a research grant of the W. M. Keck Foundation.

-
- [1] J. K. Jain, Phys. Rev. Lett. 63 (1989) 199.
 - [2] O. Heinonen, ed., *Composite fermions: a unified view of the quantum Hall regime* (World Scientific, 1998).
 - [3] B. I. Halperin, P. A. Lee, and N. Read, Phys. Rev. B 47 (1993) 7312.
 - [4] V. Kalmeyer and S.-C. Zhang, Phys. Rev. B 46 (1992) 9889.
 - [5] A. Lopez and E. Fradkin, Phys. Rev. B 44 (1991) 5246.
 - [6] A. Lopez and E. Fradkin, Phys. Rev. B 47 (1993) 7080.
 - [7] R. Du, H. Stormer, D. Tsui, L. Pfeiffer, and K. West, Phys. Rev. Lett. 70 (1993) 2944.
 - [8] S. H. Simon and B. I. Halperin, Phys. Rev. B 48 (1993) 17368.
 - [9] K. Park and J. K. Jain, Phys. Rev. Lett. 80 (1998) 4237; Solid State Comm. 119 (2001) 291.
 - [10] G. Murthy, Phys. Rev. B 60 (1999) 13702.
 - [11] S. S. Mandal and J. K. Jain, Phys. Rev. B 63 (2001) 201310.
 - [12] M. Onoda, T. Mizusaki, and H. Aoki, Phys. Rev. B 64 (2001) 235315.
 - [13] C. Kallin and B. I. Halperin, Phys. Rev. B 30 (1984) 5655.
 - [14] F. D. M. Haldane and E. H. Rezayi, Phys. Rev. Lett. 54 (1985) 237.
 - [15] S. M. Girvin, A. H. MacDonald, and P. M. Platzman, Phys. Rev. Lett. 54 (1985) 581.
 - [16] A. Pinczuk, B. S. Dennis, L. N. Pfeiffer, and K. W. West, Phys. Rev. Lett. 70 (1993) 3983.
 - [17] A. Pinczuk, L. L. Sohn, B. S. Dennis, L. N. Pfeiffer, and K. W. West, Bull. Am. Phys. Soc. 40 (1995) 515.
 - [18] H. D. M. Davies, J. C. Harris, J. F. Ryan, and A. J. Turberfield, Phys. Rev. Lett. 78 (1997) 4095.
 - [19] S. D. Sarma and A. Pinczuk, eds., *Perspectives in Quantum Hall Effects* (Wiley, New York, 1997).
 - [20] J. C. Harries, H. D. M. Davies, J. F. Ryan, and A. J. Turberfield, Physica B 258 (1998) 44.
 - [21] M. Kang, A. Pinczuk, B. S. Dennis, M. A. Eriksson, L. N. Pfeiffer, and K. W. West, Phys. Rev. Lett. 84 (2000) 546.
 - [22] M. Kang, A. Pinczuk, B. S. Dennis, L. N. Pfeiffer, and K. W. West, Phys. Rev. Lett. 86 (2001) 2637.
 - [23] V. W. Scarola, K. Park, and J. K. Jain, Phys. Rev. B 61 (2000) 13064.
 - [24] I. Dujovne, A. Pinczuk, M. Kang, B. S. Dennis, L. N. Pfeiffer, and K. W. West, Phys. Rev. Lett. 90 (2003)

- 036803.
- [25] I. Dujovne, A. Pinczuk, M. Kang, B. S. Dennis, L. N. Pfeiffer, and K. W. West, work in progress (2003).
 - [26] T. Chakraborty, *Adv. Phys.* 49 (2000) 959.
 - [27] J. Longo and C. Kallin, *Phys. Rev. B* 47 (1993) 4429.
 - [28] T. Nakajima and H. Aoki, *Phys. Rev. Lett.* 73 (1994) 3568.
 - [29] A. Lopez and E. Fradkin, *Phys. Rev. B* 51 (1995) 4347.
 - [30] S. S. Mandal and J. K. Jain, *Phys. Rev. B* 64 (2001) 125310.
 - [31] W. Pan, H. L. Stormer, D. C. Tsui, L. N. Pfeiffer, K. W. Baldwin, and K. W. West, *Phys. Rev. Lett.* 90 (2003) 016801.
 - [32] V. W. Scarola, J. K. Jain, and E. H. Rezayi, *Phys. Rev. Lett.* 88 (2002) 216804.
 - [33] I. Szlufarska, A. Wójs, and J. J. Quinn, *Physica E* 12 (2002) 59.
 - [34] A. Pinczuk, J. P. Valladares, D. Heiman, A. C. Gossard, J. H. English, C. W. Tu, L. N. Pfeiffer, and K. W. West, *Phys. Rev. Lett.* 61 (1988) 2701.
 - [35] I. K. Marmorkos and S. D. Sarma, *Phys. Rev. B* 45 (1992) 13396.
 - [36] W. Kang, J. B. Young, S. T. Hannahs, E. Palm, K. L. Campman, and A. C. Gossard, *Phys. Rev. B* 56 (1997) 12776.
 - [37] I. V. Kukushkin, K. v. Klitzing, and K. Eberl, *Phys. Rev. Lett.* 82 (1999) 3665.
 - [38] A. Pinczuk, B. S. Dennis, D. Heiman, C. Kallin, L. Brey, C. Tejedor, S. Schmitt-Rink, L. N. Pfeiffer, and K. W. West, *Phys. Rev. Lett.* 68 (1992) 3623.
 - [39] W. Pan, H. L. Stormer, D. C. Tsui, L. N. Pfeiffer, K. W. Baldwin, and K. W. West, *Phys. Rev. Lett.* 88 (2002) 176802.
 - [40] I. Szlufarska, A. Wójs, and J. J. Quinn, *Phys. Rev. B* 64 (2001) 165318.